

THE SOLUTION OF A SOLID BODY AT ITS HORIZONTAL SURFACE, GOVERNED BY FREE CONVECTIVE CELLULAR MOTION

PAVEL HRMA and IVAN BĚLOHOUBEK

Joint Laboratory for Silicate Chemistry of the Czechoslovak Academy of Sciences and the University of Chemical Technology, Prague, Czechoslovakia

(Received 11 January 1972 and in revised form 17 July 1972)

Abstract—Using the integral balance method the relation for the rate of solution of the horizontal surface of a solid body in a liquid is derived. The dissolution is governed by the free convection with a cellular motion. As starting relations the mass balance of the dissolved substance and the total mass balance, both in the cell volume limited by the phase boundary and a reference plane parallel to it, are used. The equation which expresses the mass conservation law for the dissolved substance when crossing the phase boundary, and the Navier–Stokes equation in the Boussinesq approximation, written for the stationary state with negligible inertial term, are also employed. The resulting relation for the dissolution rate is yielded in the form: $Nu = BRa^{\frac{1}{3}}$, where B is a constant having a value from 0.13 to 0.15. This relation was tested experimentally for three systems: rock salt monocrystal–water, blue vitriol monocrystal–water, and compact polycrystalline mixture of $\text{NaNO}_2 + \text{KNO}_3$ –water. The dissolution was found to be governed by the cellular convection with the mean ratio $Nu/Ra^{\frac{1}{3}}$ equal to 0.151 ± 0.014 . This value is in good agreement with the theoretical estimation.

NOMENCLATURE

A ,	size of the horizontal cross section area of the cell;	Nu ,	Nusselt number;
B ,	dimensionless constant, equations (11), (12) and (32);	Ra ,	Rayleigh number;
c ,	concentration;	S ,	area;
D ,	diffusion coefficient;	u ,	velocity of convection;
$E(\xi)$,	dimensionless function, equation (27) ₂ ;	v ,	rate of dissolution;
$f(\eta/H)$,	dimensionless function equation (14);	w ,	mass fraction;
$g(\xi)$,	dimensionless function, equation (14);	x ,	horizontal coordinate;
g ,	acceleration due to gravity;	X ,	characteristical horizontal length;
$G(\xi)$,	dimensionless function, equation (22) ₁ ;	y ,	vertical coordinate;
I ,	dimensionless integral, equation (10) ₁ ;	Y ,	distance of the reference plane from the phase boundary;
j ,	mass flux density;	z ,	distance from the leading edge;
J ,	dimensionless integral, equation (10) ₂ ;	α ,	dimensionless quantity, equation (15) ₁ ;
L ,	dimensionless integral, equations (22) ₂ and (27) ₁ ;	γ ,	dimensionless concentration, equation (5) ₄ ;
		$\bar{\gamma}$,	mean dimensionless concentration, equation (10) ₃ ;
		$\Delta\gamma$,	dimensionless concentration difference;
		δ ,	dimensionless quantity, equation (15) ₂ ;

- ε , $(1 - w_0(\partial\rho/\partial c)_{c=c_0})/(1 - w_0)$;
 η , dimensionless vertical coordinate, equation (5)₂;
 H , dimensionless distance of the reference plane from the phase boundary, equation (5)₃;
 ξ , dimensionless horizontal coordinate, equation (5)₁;
 μ , dynamic viscosity;
 ν , kinematic viscosity;
 ρ , density;
 φ , dimensionless velocity, equation (5)₅.

Subscripts

- o , phase boundary;
 ∞ , bulk;
 H , hexagonal cell;
 R , roll cell;
 s , solid phase.

INTRODUCTION

IF AN infinite horizontal surface of a solid body is dissolved in a stagnant liquid, and an inverse density gradient is produced by the concentration field, cellular convection occurs in the liquid [1]. In a wide range of dissolution rates the cells are laminar at the neighbourhood of the phase boundary, and do not change their positions with time. The shape of the cells can be hexagonal or that of rolls.

Most of the theoretical and experimental studies concerning cellular convection are confined to the case of the heat transfer through a thin horizontal liquid layer heated from below. A boundary layer theory for the cellular motion has also been worked out, but its validity is restricted to Prandtl numbers approaching to one in the case of rigid boundaries [2].

However, mass transfer under cellular convection is no less technologically important than heat transfer and, from the experimental point of view, it has some advantages: measurement of mass transfer velocity is relatively easy,

and the traces of cells remain visible on the corrosion relief as a network of cavities.

In this study the problem is theoretically solved by the integral balance method. The total mass balance and the balance of the dissolved substance are expressed for a part of the cell bounded by the surface of the dissolved body and the reference plane lying in the given distance from this surface. The balance of momentum is expressed by the Boussinesq approximation of the Navier–Stokes equation, in which the inertial term is neglected.

The experiments are carried out in such a way that the lower horizontal surface of a solid body is dissolved in a large volume of liquid at a constant temperature. The body and the liquid are selected so as to ensure that the density of the solution increases with increasing concentration of the dissolved substance.

THEORETICAL

The vertical cross-section of a cell is schematically shown in Fig. 1. The dissolved body is placed above and the liquid below the phase boundary (the strong arched line). There are introduced coordinates x and y with an origin located in the point of intersection of the cell axis with the phase boundary; the y -axis is vertical and is directed from the phase boundary into the bulk; the x -axis is perpendicular to it. The half breadth of the cell is denoted by X . In the distance Y a plane parallel to x -axis is shown

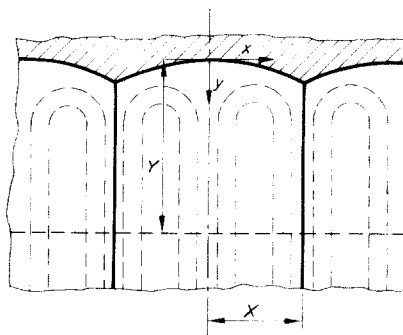


FIG. 1. Scheme of a cell.

which bounds a volume for the integral balances in the upper part of a cell.

For simplicity the following binary system is considered: the dissolved solid as a single-component and the liquid consisting of two components one of which being identical with that of the dissolved solid. The phase boundary is impervious to the liquid and no chemical reaction proceeds between the two components. The dissolution is consequently governed by a diffusion in the liquid phase and the solution on the phase boundary is saturated. A stationary state and zero heat of dissolution is assumed, and hence the density gradient is determined only by the concentration field.

Since the shapes of the cavities remain unchanged in the stationary state, the vertical velocity of dissolution remains constant and can be expressed by the relation (for the derivation of which see Appendix):

$$v = - \frac{\epsilon D}{\rho_s A} \int_A \left. \frac{\partial c}{\partial y} \right|_{y=0} dS \quad (1)$$

where $\epsilon \equiv (1 - w_0(\partial\rho/\partial c)_{c=c_0})/(1 - w_0)$, w_0 is the saturated mass fraction of the dissolved substance, ρ is the local density of the solution, ρ_s is the apparent density of the dissolved body, c is the concentration, D is the binary diffusion coefficient, dS the element of the area and A is the area size of the phase boundary belonging to one cell.

Total mass balance and the mass balance of the dissolved substance may be written for a volume bounded by the phase boundary, the vertical walls of the cell and the plane $y = Y$. In the stationary state the total mass of the liquid and the mass of the dissolved substance both passing across the surface of this volume and equal to zero. No mass passes the vertical walls because of a zero horizontal velocity component, and a symmetric maximum or minimum concentration on these walls. If neglecting the mass of the dissolved substance crossing the phase boundary, as compared with the total mass flow through the $y = Y$ plane, the continuity equation

becomes simply

$$\int_A u \, dS = 0. \quad (2)$$

The dissolved substance crosses both the phase boundary and the plane $y = Y$, hence

$$D \int_A \left. \frac{\partial c}{\partial y} \right|_{y=0} dS + \int_A cu \, dS = 0. \quad (3)$$

The flux of the dissolved substance resulting from diffusion is neglected as compared with that for the convection on the plane $y = Y$. In equations (2) and (3) u is the value of the vertical velocity component of the convection. The area of the plane belonging to one of the cells is assumed equal to A which is valid when the cell-cavity depth is small in comparison to its breadth.

The balance of momentum can be expressed by the Boussinesq approximation. In the neighbourhood of the phase boundary the convection is very slow and the inertial term can be neglected. The equation of motion for the vertical velocity component can be written as follows:

$$\mu \nabla^2 u = \frac{\partial \rho}{\partial c} g(c - \bar{c}) \quad (4)$$

where $\bar{c} \equiv 1/A \int_A c \, dS$ is the mean concentration at the plane $y = Y$. The dimensionless length, the concentration and the vertical velocity component are defined by the relations:

$$\xi \equiv x/X, \quad \eta \equiv y/Y, \quad H \equiv Y/X$$

$$\gamma \equiv (c_0 - c)/(c_0 - c_\infty) \quad (5)$$

$$\rho \equiv \frac{u_u}{(\partial\rho/\partial c)(c_0 - c_\infty)gX^2}$$

The definition of dimensionless velocity ρ is based on the form of equation (4) because no reference velocity is available.

Introducing equation (5) into equations (1)–(4), after some arrangement the following equa-

tions can be obtained:

$$v = I \frac{\varepsilon D(c_0 - c_\infty)}{\rho_s X} \tag{6}$$

$$X^3 = \frac{I}{J} \frac{\mu D}{(\partial \rho / \partial c)(c_0 - c_\infty)g} \tag{7}$$

$$\int_A \varphi \, dS = 0 \tag{8}$$

$$\nabla^2 \varphi = \bar{\gamma} - \gamma \tag{9}$$

where

$$\left. \begin{aligned} I &= \frac{1}{A} \int_A \left. \frac{\partial \gamma(\xi, \eta)}{\partial \eta} \right|_{\eta=0} dS \\ J &= \frac{1}{A} \int_A \gamma(\xi, \eta) \varphi(\xi, \eta) dS \\ \bar{\gamma} &= \frac{1}{A} \int_A \gamma dS. \end{aligned} \right\} \tag{10}$$

Connection between equations (6) and (7) gives for the rate of dissolution:

$$v = B \frac{\varepsilon}{\rho_s} \left(\frac{\partial \rho}{\partial c} (c_0 - c_\infty)^4 D^2 g \mu^{-1} \right)^{\frac{1}{3}} \tag{11}$$

where

$$B = (I^2 J)^{\frac{1}{3}}. \tag{12}$$

The quantity B defined by equation (12) is only dependent on both the dimensionless concentration distribution and the dimensionless velocity distribution in the cell.

As is common in the boundary layer theory, these distributions can be expressed in the form of simple elementary functions which fulfil the boundary conditions. For the cell the following boundary conditions come into question.

On the phase boundary the solution is saturated, i.e. $c = c_0$ and

$$\gamma = 0 \text{ at } \eta = 0. \tag{i)}$$

On the vertical cell walls the horizontal velocity component is zero and the vertical velocity reaches its maximum or minimum (according

to the flow direction, up or down). The same must hold in the cell axis:

$$\partial \varphi / \partial \xi = 0 \text{ at } \xi = 0 \text{ and } \xi = 1. \tag{ii)}$$

In order to estimate the concentration and velocity distribution in the cell, the dimensionless thickness, H , must be specified in terms of these distributions. The relative concentration difference between the cell axis and the vertical cell wall $\Delta \gamma(\eta) = \gamma(1, \eta) - \gamma(0, \eta) = (c(0, y) - c(x, y)) / (c_0 - c_\infty)$ equals zero both on the phase boundary and in the bulk. It suggests to choose the distance of the reference plane, $y = Y$, from the phase boundary to have the maximum value of $\Delta \gamma(\eta)$ in the reference plane

$$\frac{\partial \Delta \gamma(\eta)}{\partial \eta} = 0 \text{ at } \eta = H. \tag{iii)}$$

Considering that in this distance the horizontal velocity component is minimum and may be assumed zero, the continuity equation gives:

$$\frac{\partial \varphi}{\partial \eta} \approx 0 \text{ at } \eta = H. \tag{iv)}$$

The case when liquid streams up along the cell axis and down along the cell walls is now dealt with in detail.

For the dimensionless concentration distribution the following function can be established.

$$\gamma(\xi, \eta) = (\alpha + \delta g(\xi)) f(\eta/H) \tag{13}$$

where functions $g(\xi)$ and $f(\eta/H)$ hold these properties:

$$g(0) = 0, \quad g(1) = 1$$

$$\frac{dg(\xi)}{d\xi} > 0 \text{ at } \xi \in \langle 0, 1 \rangle$$

$$f(0) = 0, \quad f'(1) = 0 \tag{14}$$

$$\frac{df(\eta/H)}{d(\eta/H)} > 0 \text{ at } \eta \in \langle 0, H \rangle$$

and α and δ are constants. It is easily seen that the conditions (i) and (iii) are fulfilled under

$$\alpha = \frac{\gamma(0, H)}{f(1)}, \quad \delta = \frac{\gamma(1, H) - \gamma(0, H)}{f(1)}. \tag{15}$$

In the case of a roll-cell (i.e. rectangular cell) cartesian coordinates are convenient. Then equations (8)–(10) can be written:

$$\int_0^1 \varphi(\xi, \eta) d\xi = 0 \tag{16}$$

$$\frac{d^2 \varphi(\xi, H)}{d\xi^2} = \bar{\gamma}(H) - \gamma(\xi, H) \tag{17}$$

$$\left. \begin{aligned} I_R &= \int_0^1 \left. \frac{\partial \gamma(\xi, \eta)}{\partial \eta} \right|_{\eta=0} d\xi \\ J_R &= \int_0^1 \gamma(\xi, H) \varphi(\xi, H) d\xi \\ \bar{\gamma}(H) &= \int_0^1 \gamma(\xi, H) d\xi. \end{aligned} \right\} \tag{18}$$

Equation (17) is valid under condition (iv). Introducing equation (13) into equations (17) and (18) and employing equation (16) and boundary condition (ii) it is obtained:

$$I_R = \frac{\bar{\gamma}(H) f'(0)}{H f(1)} \tag{19}$$

$$\varphi(\xi, H) = \Delta\gamma(H)G(\xi) \tag{20}$$

$$J_R = (\Delta\gamma(H))^2 L_R \tag{21}$$

where

$$\begin{aligned} G(\xi) &= \int_0^\xi \int_0^\xi g(\xi) d\xi d\xi - \int_0^1 \int_0^\xi g(\xi) d\xi d\xi \\ &\quad - \frac{1}{2}(\xi^2 - \frac{1}{3}) \int_0^1 g(\xi) d\xi \tag{22} \\ L_R &= \int_0^1 g(\xi)G(\xi) d\xi. \end{aligned}$$

The value of B_R is now:

$$B_R = (L_R(f'(0)/f(1))^{\frac{1}{2}} (\bar{\gamma}(H) \Delta\gamma(H)/H)^{\frac{1}{2}}. \tag{23}$$

In the case of hexagonal cells it is convenient to replace the hexagon by a circle of diameter equal to the length of the hexagon side. Then ξ and η can be regarded as cylindrical coordinates. Accordingly $dS = 2X^2\pi\xi d\xi$ and $A = \pi X^2$. Equations (8)–(10), rewritten for cylindrical

coordinates ξ and η , lead after an analogous manipulation to the following result:

$$I_H = \frac{\bar{\gamma}(H) f'(0)}{H f(1)} \tag{24}$$

$$J_H = (\Delta\gamma(H))^2 L_H \tag{25}$$

$$B_H = (L_H(f'(0)/f(1))^{\frac{1}{2}} (\bar{\gamma}(H) \Delta\gamma(H)/H)^{\frac{1}{2}} \tag{26}$$

where

$$L_H = 2 \int_0^1 g(\xi) E(\xi) \xi d\xi \tag{27}$$

$$\begin{aligned} E(\xi) &= \int_0^\xi \int_0^\xi g(\xi) \xi d\xi d\xi - 2 \int_0^1 \xi \int_0^\xi \frac{1}{\xi} \int_0^\xi \\ &\quad \times g(\xi) \xi d\xi d\xi d\xi - \frac{1}{2}(\xi^2 - \frac{1}{2}) \int_0^1 g(\xi) \xi d\xi. \end{aligned}$$

In accordance with experience B can be assumed as a constant independent of the Rayleigh number value. However, it is seen from equations (6) and (7) that the integrals I and J need not be constant. It is known that the cell size X decreases very slightly with increasing Ra [3]. Considering for the sake of simplicity X as a constant and defining

$$Ra_X = (\partial\rho/\partial c) (c_0 - c_\infty) gX^3/\mu D$$

and

$$Nu_X = v\rho_s X / (\epsilon D(c_0 - c_\infty)),$$

the integrals $I = Nu_X$ and $I/J = Ra_X$ may vary with the concentration difference $(c_0 - c_\infty)$ and thus with the rate of dissolution v at a given system. On using equations (19), (21) and (23) or (24)–(26) the numbers

$$Nu_X = (\bar{\gamma}(H)/H) (f'(0)/f(1))$$

and

$$Ra_X^{\frac{1}{2}} = B_H^{\frac{1}{2}} / (L_H^{\frac{1}{2}} \Delta\gamma(H))$$

are yielded. From this it can be concluded that, if the horizontal cell size X is constant, the ratio of the relative mean concentration at

$\eta = H$ to the dimensionless eddy layer thickness $\bar{\gamma}(H)/H$ increases and the maximum relative concentration difference $\Delta\gamma(H)$ decreases with the increasing rate of dissolution or with increasing Ra_x while the ratio $\bar{\gamma}(H)\Delta\gamma(H)/H$ remains constant if B is independent on Ra_x .

The experimental study of the temperature distribution in the cell in the horizontal liquid layer heated from below is due to Leontiev and Kirdyashkin [4]. They found that the ratio of the cell size to the liquid layer thickness is equal to 1 in the region of the stability loss and 2 in the region of $Ra > Ra_{cr}$. It follows that for the roll-cell $H \leq \frac{1}{2}$ (the thickness of the dimensionless liquid layer can be maximally equal $2H$) and for the hexagonal-cell $H \leq \frac{1}{4}$.

The Fig. 7, p. 1465 published by Leontiev and Kirdyashkin [4] has served to calculate $\bar{\gamma}(H) \leq 0.4$ and $\Delta\gamma(H) \leq 0.5$ for the hexagonal cell.

The constancy of B can be secured, for example, by $\bar{\gamma}(H) = \bar{\gamma}(H_1)(H/H_1)^n$ and $\Delta\gamma(H) = \Delta\gamma(H_1)(H/H_1)^{1-n}$ where H_1 refers to any reference state. If $H_1 = \frac{1}{2}$, $\bar{\gamma}(H_1) = \frac{1}{2}$ and $\Delta\gamma(H_1) = \frac{1}{2}$ is taken for the case of the roll-cell and $H_1 = 0.25$, $\bar{\gamma}(H_1) = 0.4$ and $\Delta\gamma(H_1) = 0.5$ in the case of the hexagonal cell,

$$(\bar{\gamma}(H)\Delta\gamma(H)/H) = (\bar{\gamma}(H_1)\Delta\gamma(H_1)/H_1)$$

and equals 0.5 and 0.8 for roll and hexagonal cells respectively.

Consider the most simple model of the concentration distribution in a cell:

$$g(\xi) = \xi, \quad f(\eta/H) = \eta/H. \quad (28)$$

From equations (19) and (21)–(27) follows that

$f'(0) = 1$, $f(1) = 1$, $L_R = 1/120$, $L_H = 1/270$, $B_R = (1/480)^{\frac{1}{3}} = 0.128$ and $B_H = (0.64/270)^{\frac{1}{3}} = 0.133$. Taking

$$g(\xi) = \xi^2, \quad f(\eta/H) = \eta/H \quad (29)$$

then $B_R = 0.128$ and $B_H = 0.149$. These two values for hexagonal cells coincide well with the empirical formulas for the heat transfer from the downward-facing horizontal surfaces. For example Fishenden [5] reports the relationship $Nu = 0.14 Ra^{\frac{1}{3}}$.

THE PROPERTIES OF THE USED SYSTEMS

For the investigation of the cellular convection there were used single crystals of blue vitriol, single crystals of rock salt and a compact polycrystalline mixture of NaNO_2 and KNO_3 with the weight ratio 1:0.807; these substances were dissolved in their aqueous solutions of different concentrations at 20°C.

The physical properties of blue vitriol and rocksalt and their aqueous solutions are available in the literature [5, 6] and listed in Table 1.

The physical properties of the mixture $\text{NaNO}_2 + \text{KNO}_3$ of weight ratio 1:0.807 and its aqueous solutions had to be measured. They are listed in the last row of Table 1.

For the weight ratio 1:0.807 both components in their aqueous solution are in phase equilibrium with the two corresponding crystal phases at 20°C. The weight concentration of NaNO_2 and KNO_3 in this saturated aqueous solution was first determined after Lung, titrating by KMnO_4 solution (only nitrite content) and then the total content of nitrate + nitrite by means of evaporation residue. It was reasoned that the

Table 1. Properties of the systems used

System	Density of solid ρ_s (g/cm ³)	Saturated concentration c_0 (g/cm ³)	Diffusion coefficient at saturated concentration $D_0 \times 10^9$ (cm ² /s)	Viscosity of solution $\nu \cdot 10^2$ (cm ² /s)	Density of solution ρ (g/cm ³)
$\text{CuSO}_4 \cdot 5\text{H}_2\text{O} - \text{H}_2\text{O}$	2.286	0.326	0.33	$1.004 + 2.420c$	$0.9882 + 0.6424c - 0.0904c^2$
$\text{NaCl} - \text{H}_2\text{O}$	2.163	0.317	1.4	$1.004 + 0.653c + 3.456c^2$	$0.9982 + 0.687c - 0.154c^2$
$(\text{NaNO}_2 + \text{KNO}_3) - \text{H}_2\text{O}$	2.146	0.990	3.02	$1.004 + 3.170c^3$	$0.9982 + 0.565c$

ratio found should ensure the most uniform dissolution of the polycrystalline compact mixture formed by the same ratio of both components.

The densities of the solutions were measured pycnometrically and the viscosities of the solutions were measured by the Ubbé's tube viscosimeter.

The diffusion coefficient was calculated from the data of dissolution of a vertical cylindrical specimen under conditions of the density free convection along with the following formula:

$$v = 0.490 \varepsilon \frac{c_0 - c_\infty}{\rho_s} \left(\frac{(\rho_0 - \rho_\infty) g D_0^3}{\mu_0 z} \right)^{\frac{1}{4}} \quad (30)$$

The dissolution rate, v , was measured at five concentrations, c_∞ , within the range 0.62–0.87 g/cm³. From the slope of the dependence $vz^{\frac{1}{4}}$ on $((c_0 - c_\infty)/\rho_s) ((\rho_0 - \rho_\infty)/\mu_0)^{\frac{1}{4}}$, found by the last square method, the effective binary diffusion coefficient, D_0 , was obtained.

THE MEASURING OF THE RATE OF DISSOLUTION

The magnitudes of the dissolved surface area of single crystals laid within the range of 1.5–4 cm². In the case of blue vitriol single crystals surfaces of the Miller's indexes [110] and/or $-\bar{1}\bar{1}0$ were chosen. The specimens of the NaNO₂ + KNO₃ mixture were prepared by pouring the melt into preheated glass rings placed on glass plates followed by careful cooling.

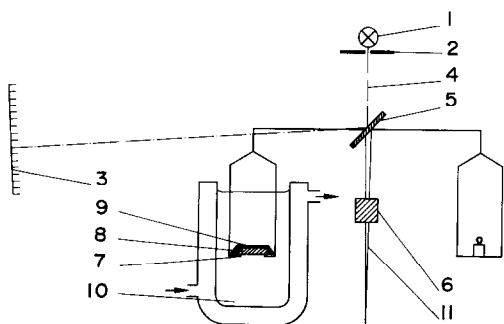


FIG. 2. Scheme of the apparatus for the measurement of the dissolution rate.

The resulting tablets were compact and their surfaces were perfectly smooth. The surface areas used for the dissolution experiments were of a mean magnitude 6 cm².

The range of concentrations for the solutions used in dissolution experiments was relatively wide: from pure water up to $(c_0 - c_\infty) \approx 10^{-2}$ g/cm³. The dissolution rate was measured on an adapted sedimentation balance (Fig. 2). The part of surface of single crystal or tablet 8 which was not assigned for dissolution was isolated by paraffin wax 9 served at the same time for the connection of the dissolved body with the annulus 7 of the balance beam.

The isolation was made in such a way that the single crystals were put on a glass plate, with their surfaces intended for dissolution faced downwards, and embedded by molten paraffin wax. In the case of polycrystalline samples the surfaces intended for dissolution were protected by a rubber sucker and the samples were submerged into paraffin wax melt. The edges of unprotected surfaces were subsequently adapted by organic plasticine.

The polycrystalline surfaces intended for dissolution had circular shapes, and those of blue vitriol were in rhomboedrical or rectangular shapes. In the case of the rock salt the shapes of these surfaces varied to some extent with different samples.

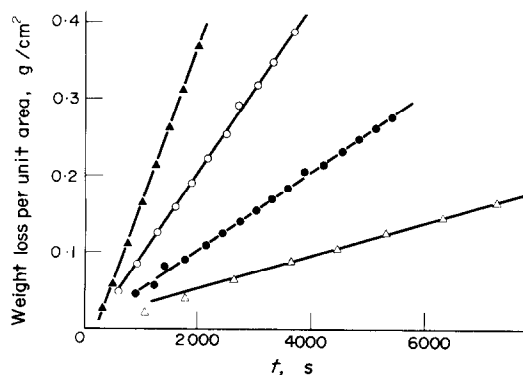


FIG. 3. Time-dependence of the mass loss of NaNO₂ + KNO₃ specimens at their dissolution in solutions of the following concentrations in g/cm³: 0.806 (▲), 10.850 (○), 0.900 (●), and 0.927 (△).

The solution 10 was held at the temperature $20 \pm 0.1^\circ\text{C}$ under tempering bathing. The change of the balance sensitivity was realized by the weight 6 moving on the tongue of the balance 11. The luminous ray from the light source 1 passed through the diaphragm 2, rebounded from the mirror 5 attached on the tongue, and impinged into the screen 3 equipped with a scale from which the weight loss of the dissolved body was read off.

The value of the mass flux density j_0 was calculated from the linear part of the time dependence of the weight loss per unit area by the last square method. An example of such a dependence is shown in Fig. 3.

EXPERIMENTAL RESULTS AND DISCUSSION

Taking the logarithm of equation (11) and using relations $j_0 = \rho_s v$ and $\partial\rho/\partial c \approx (\rho_0 - \rho_\infty)/(c_0 - c_\infty)$ gives:

$$\log \frac{j_0}{\varepsilon D_0 (c_0 - c_\infty)} = \frac{1}{3} \log \frac{(\rho_0 - \rho_\infty) g}{\mu_\infty D_0} + \log B. \quad (31)$$

Since the viscosity and the diffusion coefficient are not independent of concentration, the bulk viscosity, μ_∞ , and the diffusion coefficient of the saturated solution, D_0 , were used. Equation (31) is suitable for testing of equation (11) by means of experimental results.

On Fig. 4 the term $j_0/\varepsilon D_0(c_0 - c_\infty)$ is plotted vs. the term $(\rho_0 - \rho_\infty)g/\mu_\infty D_0$ both in the logarithmical scale. It is evident that the line with a slope equal to $\frac{1}{3}$ is in good agreement with the experimental points. It should be noted that the complex quantities used are not dimensionless, namely the former is equal to the Nusselt number divided by the characteristic length and the later equals the Rayleigh number divided by the third power of the same characteristic length. Regarding to the exponent $\frac{1}{3}$ the characteristic length has no particular meaning and so equation (31) becomes consequently equivalent to the relation:

$$Nu = B Ra^{\frac{1}{3}}. \quad (32)$$

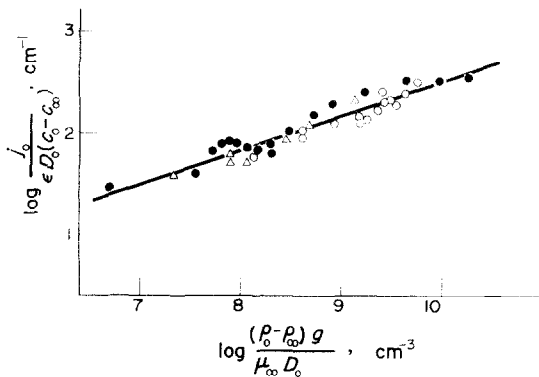


FIG. 4. The dependence of $j_0/\varepsilon D_0(c_0 - c_\infty)$ on $(\rho_0 - \rho_\infty)g/\mu_\infty D_0$ for the mixtures $\text{NaNO}_2 + \text{KNO}_3$ (●), monocrystals $\text{CuSO}_4 \cdot 5 \text{H}_2\text{O}$ (○) and NaCl (△).

The mean value of B calculated as a ratio

$$\left(\frac{j_0}{\varepsilon D_0 (c_0 - c_\infty)} \right) : \left(\frac{(\rho_0 - \rho_\infty) g}{\mu_\infty D_0} \right)^{\frac{1}{3}}$$

is 0.151 ± 0.014 for all measurements; if calculated for separate systems, then B for the blue vitriol is 0.137, for the rock salt is 0.141 and for the mixture of $\text{NaNO}_2 + \text{KNO}_3$ is 0.165. Figure 5 shows that B is a constant over the whole range of concentration used.

The dissolved surface developed corrosion reliefs showing the cellular character of the convection in the liquid. The most distinct corrosion cavities were observed on the surfaces of the monocrystals (Figs. 6 and 7). When dissolving in pure water or dilute solutions the pattern is hexagonal, though the shape of

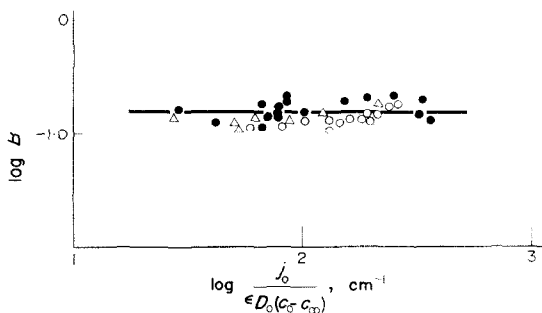


FIG. 5. Dependence of B on $j_0/\varepsilon D_0(c_0 - c_\infty)$.

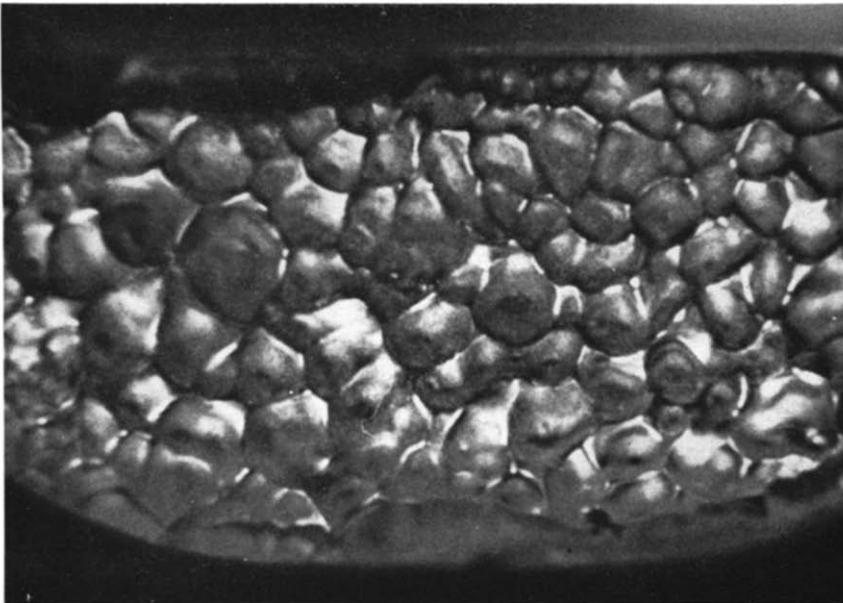


FIG. 6. The corrosion relief of NaCl, $c_0 - c_\infty = 0.317 \text{ g/cm}^3$, mgt. $8 \times$.



FIG. 7. The corrosion relief of NaCl, $c_0 = c_{\infty} = 0.010 \text{ g/cm}^3$, mgt. 5

cavities is considerably irregular. The pattern changes if the magnitude of the term $(\rho_0 - \rho_\infty)g/\mu_\infty D_0$ falls under the value of 1 to $4 \cdot 10^{+8} \text{ cm}^{-3}$ and exhibits then a dependence on the shape of the dissolved area. The cell shape is that of rolls lying perpendicular to the normal direction and pointing to the centre of the dissolved area. If the shape of the dissolved surface is circular, the shapes of roll cells are wedgewise and not rectangular deviating therefore from the assumption given in the theoretical part. This discrepancy, however, is not that important because the dissolved surface area is large. No dependence of the cell size X vs the term

$$j_0/\varepsilon D_0(c_0 - c_\infty) \quad \text{or} \quad (\rho_0 - \rho_\infty)g/\mu_\infty D_0$$

was possible to establish. The mean diameter $2X$ of a hexagonal cell was about 0.06–0.10 cm and the mean width of a roll was about 0.06–0.16 cm. That supports the assumption made in the theoretical part that X can be regarded as a constant. The estimation of the values of the maximum relative concentration difference, $\Delta\gamma(H)$, and that of the dimensionless eddy layer thickness, H , were also attempted. Choosing the value $(\rho_0 - \rho_\infty)g/\mu_\infty D_0 = 2 \cdot 10^8 \text{ cm}^{-3}$ from the period of transition between rolls and hexagons and $X \approx 0.03 \text{ cm}$, then $Ra_X = 2 \cdot 10^8 \cdot 0.03^3 = 5400$ and $\Delta\gamma(H) = (B/L)^{\frac{1}{2}} Ra_X^{-\frac{1}{2}} \approx (0.14 \cdot 270)^{\frac{1}{2}} \cdot 5400^{-\frac{1}{2}} \approx 0.35$. The Nusselt number $Nu_X = B Ra_X^{\frac{1}{2}} \approx 0.14 \cdot 5400^{\frac{1}{2}} \approx 2.5$ and $H = (f(1)/f'(0))(\bar{\gamma}(H)/Nu_X) \approx 0.4/2.5 = 0.16$. These results are in good agreement with estimations $\Delta\gamma(H) \leq 0.5$ and $H \leq 0.25$ which were used in the theoretical part.

REFERENCES

1. S. CHANDRASEKHAR, *Hydrodynamic and Hydromagnetic Stability*. Oxford University Press (1961).
2. J. L. ROBINSON, The failure of a boundary layer model to describe certain cases of cellular convection, *Int. J. Heat Mass Transfer* **12**, 1257–1265 (1969).
3. E. L. KSCHMIEDER, On convection under an air surface, *J. Fluid. Mech.* **30**, 9–15 (1967).
4. A. J. LEONTIEV and A. G. KIRDYASHKIN, Experimental study of flow patterns and temperature fields in horizontal free convection liquid layers, *Int. J. Heat Mass Transfer* **11**, 1461–1466 (1968).
5. M. FISHENDEN and O. A. SAUNDERS, *Heat Transfer*, p. 129. Oxford Press, New York (1950).
6. *International Critical Tables*. McGraw-Hill, New York (1928–1930).
7. LANDOLT-BÖRNSTEIN, *Zahlenwerte u. Funktionen*, Band II., Teil 5a, *Transportphenomäne I., Viskosität und Diffusion*. Springer, Berlin (1969).
8. A. R. COOPER, JR., Modification of Noyes–Nernst equation, *J. Chem. Phys.* **38**, 284–285 (1963).

APPENDIX

The Mass Transfer Rate at the Moving Boundary

Equation (1) expresses the mass conservation law for the dissolved substance at its transition from the solid to the liquid phase. It is valid for the system in which the solid phase is single-component and the liquid is composed by two components, one of them being identical with that of the dissolved substance; the dissolution is governed by the diffusion in the liquid phase.

In the infinitesimal liquid layer on the phase boundary the longitudinal convection can be neglected. In this layer only the diffusion and the cross convection due to the phase boundary motion occur. The continuity equation for the dissolved substance takes therefore the form:

$$v\rho_s = j_0 = -D_0(\partial c/\partial y)_{y=0} + u_y c_0 \quad (33)$$

where c is the concentration of the dissolved substance in the liquid and ρ is the liquid density. The boundary is impermeable for the other liquid component and so

$$0 = -D_0\partial(\rho - c)/\partial y|_{y=0} + u_y(\rho_0 - c_0). \quad (34)$$

The diffusion coefficients D_0 are the same in both equations (33) and (34) because the case of binary diffusion is discussed. u_y is the velocity related to the unmoving coordinates with which the liquid follows the moving boundary.

Eliminating u_y from equations (33) and (34) one obtains:

$$j_0 = -D_0(\partial c/\partial y)_{y=0}((1 - w_0\rho'_0)/(1 - w_0)) \quad (35)$$

where $w = c/\rho$ is the mass fraction of the dissolved substance and $\rho'_0 = (\partial\rho/\partial c)_{c=c_0}$. Relation (1) is so derived.

Using the well-known thermodynamical relation for the partial specific volume

$$\bar{V} = 1/\rho + (1 - w)(\partial(1/\rho)/\partial w) \quad (36)$$

where \bar{V} is the partial specific volume of the dissolved substance, carrying out the arrangement

$$\begin{aligned} \partial(1/\rho)/\partial w &= \partial(1/\rho)/\partial(c/\rho) \\ &= -(1/\rho)(\partial\rho/\partial c)/(1 - w(\partial\rho/\partial c)) \end{aligned} \quad (37)$$

consequently

$$\partial\rho/\partial c = (1 - \bar{V}\rho)/(1 - \bar{V}c) \quad (38)$$

one obtains after introducing the last relation into equation (35):

$$j_0 = -D_0(\partial c/\partial y)_{y=0}/(1 - \bar{V}_0 c_0) \quad (39)$$

which is the relation found by Cooper [5] by a different method.

Using another arrangement

$$\begin{aligned} \partial c / \partial y &= (\partial c / \partial w)(\partial w / \partial y) = (\rho / (1 - w \partial \rho / \partial c))(\partial w / \partial y) \\ &= \rho (\partial w / \partial y)(1 - \bar{V} \rho) / (1 - w) \end{aligned} \quad (40)$$

the relation (39) can be rewritten into the following form:

$$j_0 = -\rho_0 D_0 (\partial w / \partial y)_{y=0} / (1 - w_0) \quad (41)$$

which is currently used in chemical engineering.

DISSOLUTION À LA SURFACE HORIZONTALE D'UN CORPS SOLIDE GOUVERNÉE PAR LA CONVECTION NATURELLE EN MOUVEMENT CELLULAIRE

Résumé—Par la méthode du bilan intégral, on a établi la relation pour la vitesse de dissolution de la surface horizontale d'un corps solide dans un liquide. La dissolution est ici gouvernée par la convection naturelle de densité en mouvement cellulaire. On a utilisé comme relations de départ le bilan massique de la substance en dissolution et le bilan massique total appliqués tous les deux dans le volume cellulaire limité par la frontière de la phase et un plan de référence parallèle. On a employé aussi l'équation exprimant la loi de conservation de masse pour la substance dissoute traversant la frontière de la phase et l'équation de Navier-Stokes dans l'approximation de Boussinesq écrite pour l'état permanent avec un terme d'inertie négligeable. La relation résultante pour la vitesse de dissolution s'écrit sous la forme $Nu = B Ra^{\frac{1}{3}}$, B étant une constante pouvant prendre des valeurs entre 0,13 et 0,15. Cette relation a été expérimentée pour trois systèmes: monocristal de sel solide-eau, monocristal de vitriol bleu-eau et mélange polycristallin de NaNO_2 et KNO_3 -eau.

On trouve que la dissolution est gouvernée par la convection cellulaire avec le rapport moyen $Nu/Ra^{\frac{1}{3}}$ égal à $0,151 \pm 0,014$. Cette valeur est en bon accord avec l'estimation théorique.

AUFLÖSUNG EINES FESTKÖRPERS AN SEINER HORIZONTALEN OBERFLÄCHE BEI FREIER KONVEKTION IN ZELLSTRÖMUNG

Zusammenfassung—Mit der Methode des integralen Gleichgewichtes wird eine Beziehung für die Geschwindigkeit der Auflösung eines Festkörpers an seiner horizontalen Oberfläche in Flüssigkeit abgeleitet. Maßgebend für die Auflösung ist hier die freie Konvektion in Zellströmung. Ausgangsbeziehungen sind die Massengleichgewichte der gelösten Substanz und der gesamten Masse, beide in dem Zellvolumen, das durch die Phasengrenze und einer dazu parallelen Bezugsebene begrenzt wird. Eingeführt werden weiterhin die Beziehungen aus dem Massenerhaltungssatz für die gelöste Substanz beim Überschreiten der Phasengrenze, sowie die Navier-Stokes-Gleichung in der Approximation von Boussinesq für den stationären Zustand mit vernachlässigbarem Trägheitsterm. Die sich damit ergebende Beziehung hat die Form: $Nu = B Ra^{\frac{1}{3}}$, wobei B eine Konstante zwischen 0,13 und 0,15 ist. Diese Beziehung wurde für drei Systeme experimentell nachgeprüft: monokristallines Steinsalz-Wasser, monokristallines Kupfervitriol-Wasser und NaNO_2 - KNO_3 in polykristallinem Gemisch-Wasser. Es wurde gefunden, dass die Auflösung durch die Zellkonvektion mit einem mittleren $Nu/Ra^{\frac{1}{3}}$ -Verhältnis zu $0,151 \pm 0,014$ bestimmt wurde. Dieser Wert stimmt mit der theoretischen Abschätzung gut überein.

РАСТВОРЕНИЕ ГОРИЗОНТАЛЬНОЙ ПОВЕРХНОСТИ ТВЕРДОГО ТЕЛА ВСЛЕДСТВИЕ ЯЧЕЙСТОЙ СВОБОДНОЙ КОНВЕКЦИИ

Аннотация—С помощью интегрального балансного метода получено выражение для скорости растворения горизонтальной поверхности твердого тела в жидкости. Скорость растворения определяется свободной ячейистой конвекцией. В качестве исходных уравнений используются уравнения сохранения баланса массы, записанные как для объема ячейки, ограниченного границей раздела фаз, так и для плоскости сравнения параллельной ей, уравнение закона сохранения количества растворенного вещества при пересечении границы раздела и уравнение Навье-Стокса в приближении Буссинеска для стационарных условий, когда инерционный член пренебрежимо мал. Полученное уравнение для скорости растворения представлено в следующем виде: $Nu = B \cdot Ra^{\frac{1}{3}}$, где B — постоянная величина, равная $0,13 \div 0,15$. Уравнение проверялось экспериментально для трех систем: монокристалл каменной соли-вода; монокристалл медного купороса-вода; полукристаллическая смесь NaNO_2 — KNO_3 — вода. Обнаружено, что скорость растворения зависит от ячейистой конвекции, описываемой отношением $Nu/Ra^{\frac{1}{3}} = 0,151 \pm 0,014$, что хорошо согласуется с теоретическим расчетом.